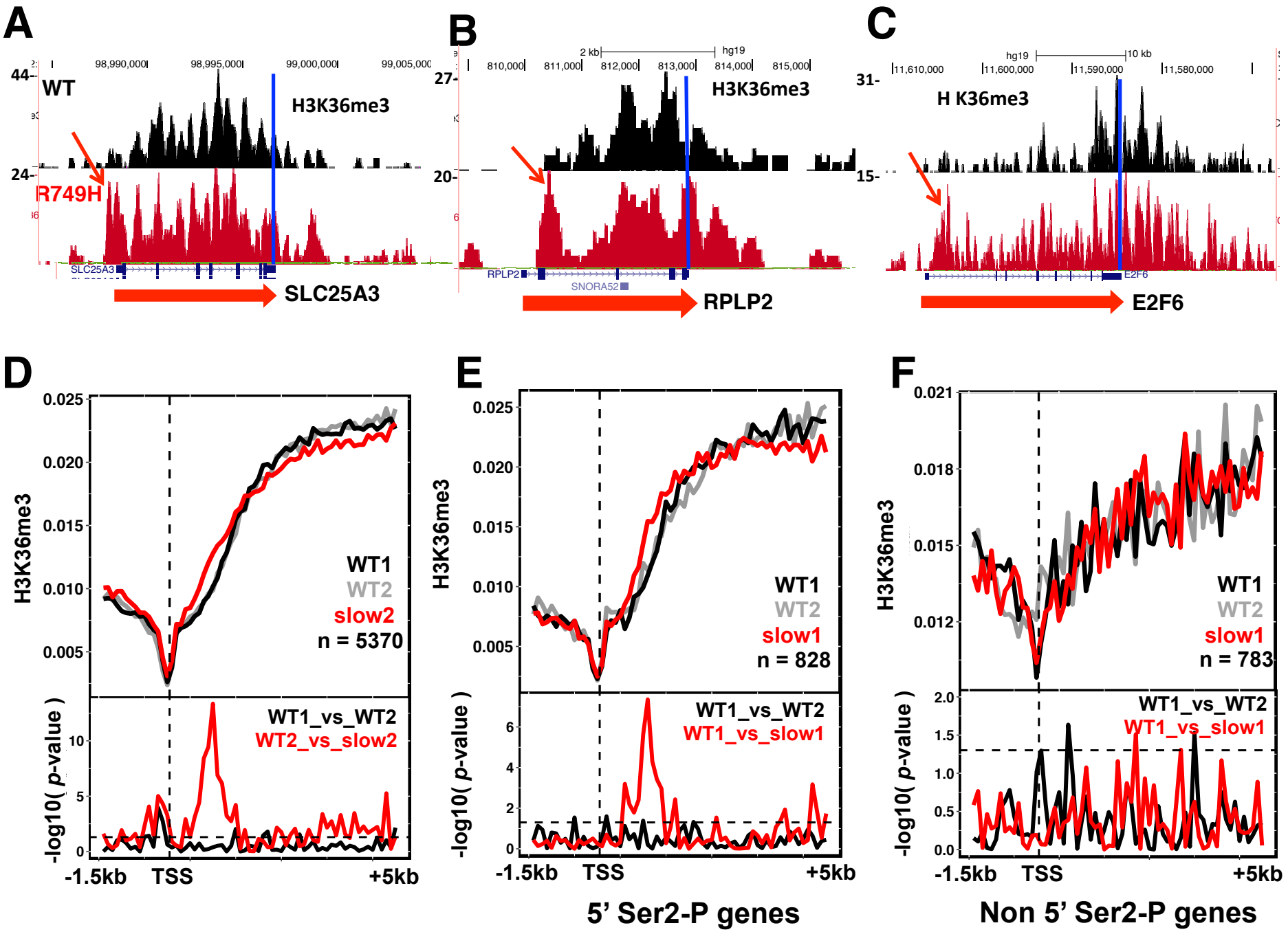
A
B
C
WT
H3K36me3
R749H
SLC25A3
RPLP2
SNORA52
E2F6
D
E
F
H3K36me3
WT1
WT2
slow2
n = 5370
slow1
n = 828
n = 783
WT1_vs_WT2
WT2_vs_slow2
WT1_vs_slow1
-log10(p-value)
-1.5kb
TSS
+5kb
5' Ser2-P genes
Non 5' Ser2-P genes

Figure S1

Figure S1. Related to Figure 2.

Slow transcription repositions H3K36me3 on human genes.

A-C. UCSC genome browser shots of H3K36me3 ChIP signals in HEK293 cells expressing WT and R749H slow pol II mutant. The results are from a biological replicate of the data in Fig. 2. Note the 5′ shift in H3K36me3 in the slow mutant (red arrows).

D. Metaplots of mean relative frequency of H3K36me3 ChIP signals in HEK293 cells expressing WT (two replicates) and R749H slow pol II mutant. 100 bp bins are shown for the region from -1.5kb to +5.0 kb relative to the TSS for a set of well-expressed genes in HEK293 cells separated by 2kb (Brannan et al., 2012). P-values (lower panel) were calculated using Welch's two sample t-test. The horizontal dotted line indicates a p-value of 0.05. Plot is of the same data set shown in A-C.

E, F. Upstream repositioning of H3K36me3 in the R749H slow mutant correlates with 5′ Ser2 hyperphosphorylation. Metaplots of mean relative frequency, as in D, of H3K36me3 ChIP signals at 5′ ends of genes with high 5′ Ser2 hyperphosphorylation in R749H (E) and in genes that are unaffected for 5′ Ser2-P (F) (Table S1). Plot is from the data set shown in Fig. 2.

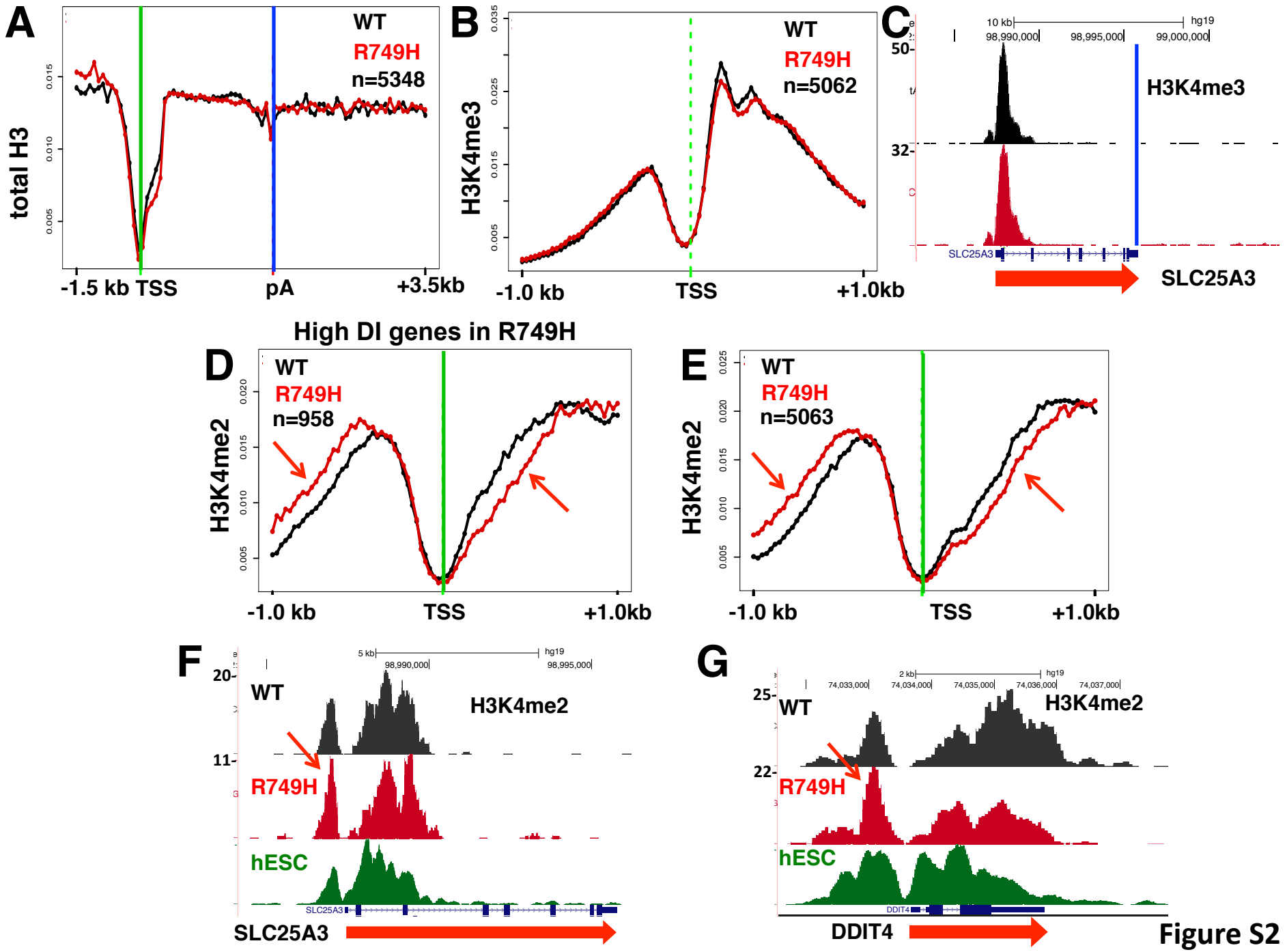
A
WT
R749H
n=5348
total H3
0.015
0.010
0.005
-1.5 kb TSS
pA
+3.5kb
B
WT
R749H
n=5062
H3K4me3
0.035
0.025
0.015
0.005
-1.0 kb
TSS
+1.0kb
C
10 kb
hg19
98,990,000
98,995,000
99,000,000
50-
32-
H3K4me3
SLC25A3
SLC25A3
High DI genes in R749H
D
WT
R749H
n=958
H3K4me2
0.020
0.015
0.010
0.005
-1.0 kb
TSS
+1.0kb
E
WT
R749H
n=5063
H3K4me2
0.025
0.020
0.015
0.010
0.005
-1.0 kb
TSS
+1.0kb
F
5 kb
hg19
98,990,000
98,995,000
20-
11-
WT
H3K4me2
R749H
hESC
SLC25A3
SLC25A3
G
2 kb
hg19
74,033,000
74,034,000
74,035,000
74,036,000
74,037,000
25-
22-
WT
H3K4me2
R749H
hESC
DDIT4
DDIT4

Figure S2

Figure S2. Related to Figures 2, 5.

Slow transcription does not reposition total histone H3 or H3K4me3 on human genes.

A. Metaplots of total H3 ChIP signals in WT and the R749H slow mutant for over 5000 well-expressed genes separated by >2kb.

B. Metaplots of H3K4me3 ChIP signals in WT and the R749H slow mutant. Note that the H3K4me3 profile is little affected by slow elongation.

C. UCSC genome browser shot of H3K4me3 ChIP in WT and the R749H slow mutant.

D. Metaplots of H3K4me2 ChIP signals in WT and the R749H slow mutant for genes with elevated DI in R749H (Table S1). Data is from the experiment in Fig. 5G.

E. Metaplots of H3K4me2 ChIP signals in WT and the R749H slow mutant for over 5000 well-expressed genes separated by >2kb. Note that slow transcription is associated with a shift in H3K4me2 upstream and downstream of the TSS (red arrows). Data is a biological replicate of the experiment in Fig. 5G.

F, G. UCSC genome browser shots for anti-H3K4me2 in WT and R749H slow pol II mutant using homemade antibody as in E, and the ENCODE H3K4me2 track (GSM733769) of H1-hESC's using abcam (ab7766) anti-K4me2 antibody to show that the results with the two antibodies are comparable. Red arrows mark elevated H3K4me2 upstream of the TSS in the slow pol II R749H mutant.

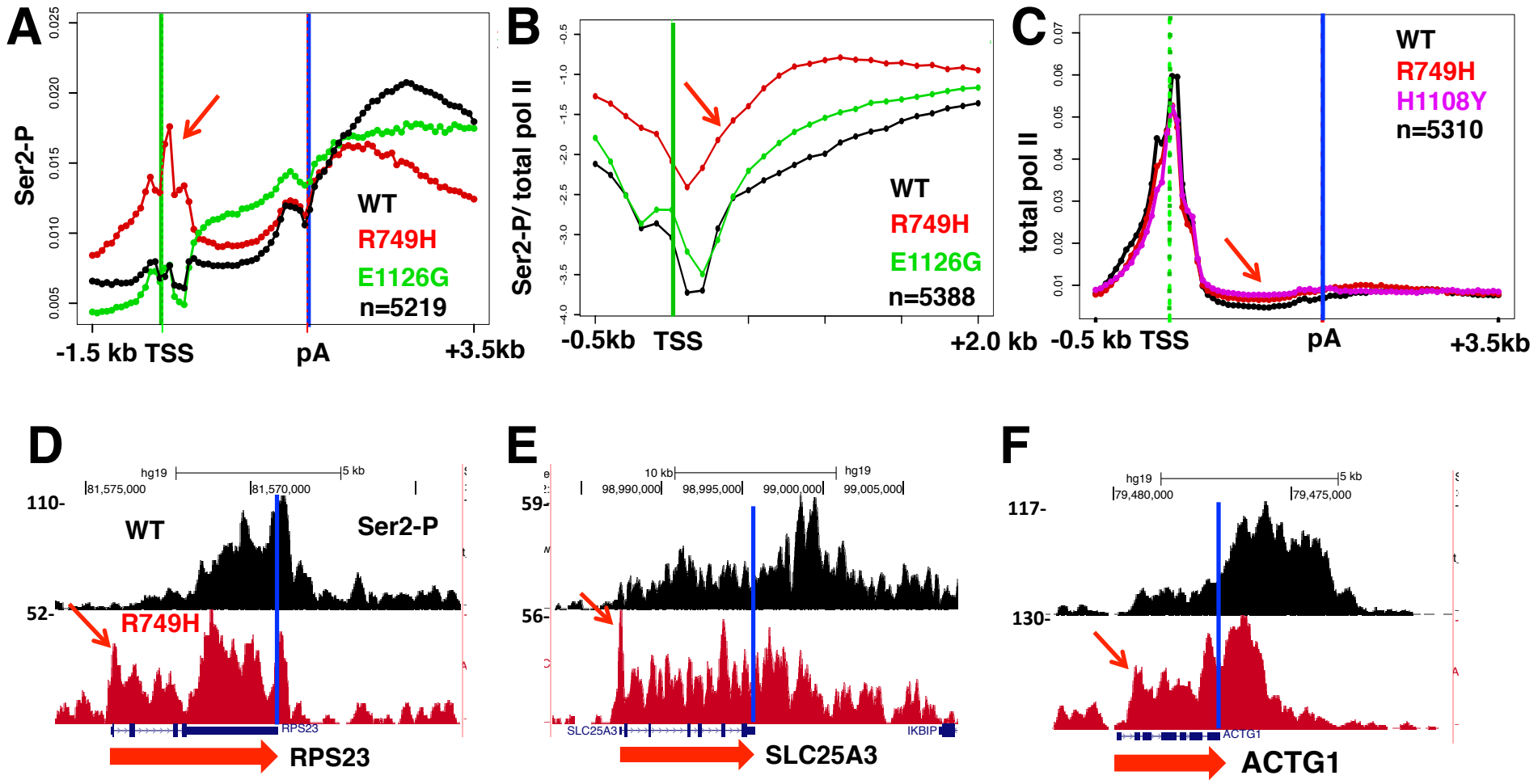
A
Ser2-P
0.025
0.020
0.015
0.010
0.005
WT
R749H
E1126G
n=5219
-1.5 kb TSS
pA
+3.5kb
B
Ser2-P/ total pol II
-0.5
-1.0
-1.5
-2.0
-2.5
-3.0
-3.5
-4.0
WT
R749H
E1126G
n=5388
-0.5kb
TSS
+2.0 kb
C
total pol II
0.07
0.06
0.05
0.04
0.03
0.02
0.01
WT
R749H
H1108Y
n=5310
-0.5 kb TSS
pA
+3.5kb
D
hg19
5 kb
81,575,000
81,570,000
110-
52-
WT
Ser2-P
R749H
RPS23
RPS23
E
10 kb
hg19
98,990,000
98,995,000
99,000,000
99,005,000
59-
56-
SLC25A3
IKBIP
SLC25A3
F
hg19
5 kb
79,480,000
79,475,000
117-
130-
ACTG1
ACTG1

Figure S3

Figure S3. Related to Figure 3.

Slow elongation causes widespread 5′ shifting of pol II CTD Ser2-P at human genes.

A. Metaplot of relative frequency of CTD Ser2-P ChIP signals for over 5000 genes in cells expressing WT, R749H slow and E1126G fast pol II mutants. Note the peak of Ser2-P at the TSS in R749H (red arrow). WT and R749H data sets are replicates of those shown in Fig. 3.

B. Metaplot of Ser2-P ChIP signals normalized to total pol II (log2) in cells expressing WT, R749H slow and E1126G fast pol II mutants. Note elevated Ser2-P around start sites in the R749H slow mutant.

C. Metaplot of relative frequency of pol II ChIP signals for over 5000 well-expressed separated by >2kb in cells expressing WT, and R749H and H1108Y slow pol II large subunit mutants. Note that relative height of peaks of paused pol II at the TSS is little affected by the rate mutants but that relative pol II density in the gene body is higher in the slow mutants (arrow) as predicted by a model relating elongation rate to pol II occupancy (Ehrensberger et al., 2013). TSS and poly(A) sites are marked by green and blue lines.

D-F Anti-Pol II CTD Ser2-P ChIP-seq shows novel 5′ peaks specific to the slow R749H mutant. UCSC genome browser screen shots with arrows marking peaks of Ser2-P near the TSSs. Results are from biological replicates of experiments shown in Fig. 3.

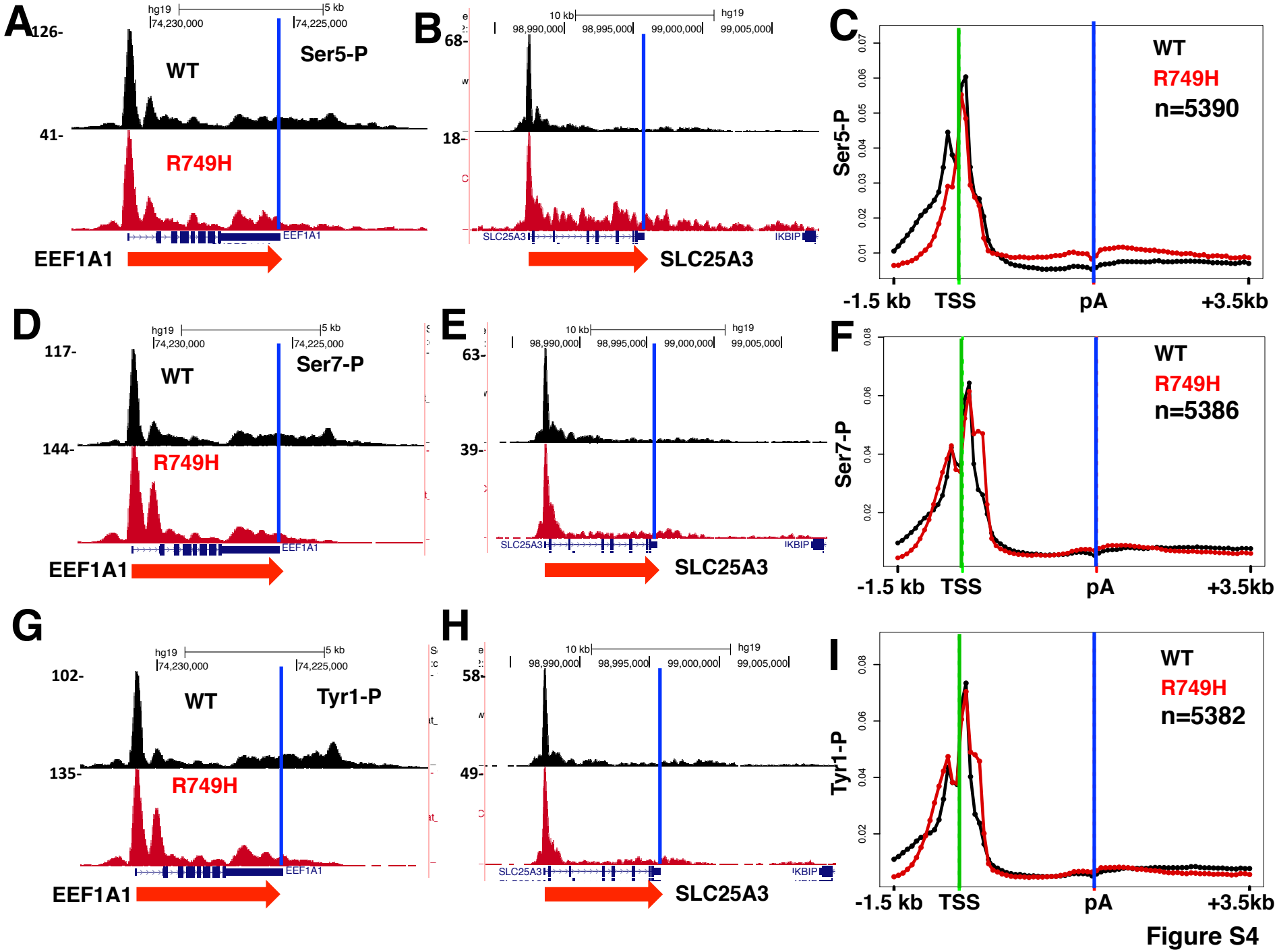
A
hg19
5 kb
74,230,000
74,225,000
126-
WT
Ser5-P
41-
R749H
EEF1A1
EEF1A1
B
10 kb
hg19
98,990,000
98,995,000
99,000,000
99,005,000
68-
18-
SLC25A3
IKBIP
SLC25A3
C
WT
R749H
n=5390
Ser5-P
0.07
0.06
0.05
0.04
0.03
0.02
0.01
-1.5 kb
TSS
pA
+3.5kb
D
hg19
5 kb
74,230,000
74,225,000
117-
WT
Ser7-P
144-
R749H
EEF1A1
EEF1A1
E
10 kb
hg19
98,990,000
98,995,000
99,000,000
99,005,000
63-
39-
SLC25A3
IKBIP
SLC25A3
F
WT
R749H
n=5386
Ser7-P
0.08
0.06
0.04
0.02
-1.5 kb
TSS
pA
+3.5kb
G
hg19
5 kb
74,230,000
74,225,000
102-
WT
Tyr1-P
135-
R749H
EEF1A1
EEF1A1
H
10 kb
hg19
98,990,000
98,995,000
99,000,000
99,005,000
58-
49-
SLC25A3
IKBIP
SLC25A3
I
WT
R749H
n=5382
Tyr1-P
0.08
0.06
0.04
0.02
-1.5 kb
TSS
pA
+3.5kb

Figure S4

Figure S4. Related to Figure 3

Transcription elongation rate does not cause major re-positioning of CTD Tyr1, Ser5, or Ser7 phosphorylation.

UCSC genome browser shots and metaplots of ChIP-seq reads for anti-CTD Ser5-P (A-C) , Ser7-P (D-F), and Tyr1-P (G-I) in WT and R749H slow pol II mutant.

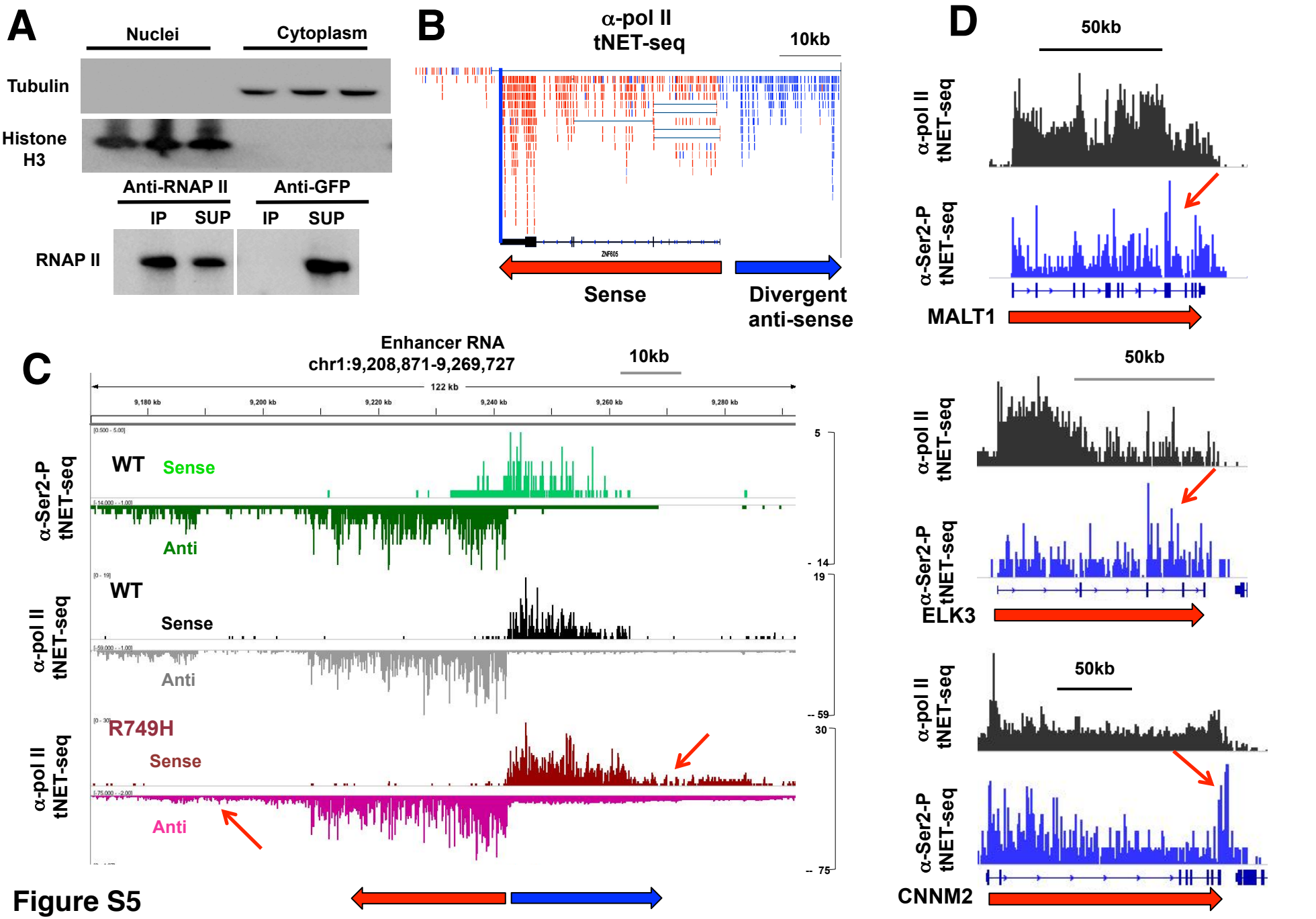
A
Nuclei
Cytoplasm
Tubulin
Histone H3
Anti-RNAP II
Anti-GFP
IP
SUP
IP
SUP
RNAP II
B
α-pol II tNET-seq
10kb
ZNF605
Sense
Divergent anti-sense
C
Enhancer RNA
chr1:9,208,871-9,269,727
10kb
122 kb
9,180 kb
9,200 kb
9,220 kb
9,240 kb
9,260 kb
9,280 kb
α-Ser2-P tNET-seq
WT
Sense
Anti
α-pol II tNET-seq
WT
Sense
Anti
α-pol II tNET-seq
R749H
Sense
Anti
5
14
19
59
30
75
D
50kb
α-pol II tNET-seq
α-Ser2-P tNET-seq
MALT1
50kb
α-pol II tNET-seq
α-Ser2-P tNET-seq
ELK3
50kb
α-pol II tNET-seq
α-Ser2-P tNET-seq
CNNM2

Figure S5

Figure S5. Related to Figure 5-7.

Nascent RNA sequencing by anti-total pol II tNET-seq and Ser2-P tNET-seq.

A. Nuclear fractionation and anti-pol II immunoprecipitation from DNAseI solubilized nuclei for tNET-seq. Top panel: Western blots of nuclear and cytoplasmic fractions with anti tubulin and H3. Bottom panel: Anti-pol II western blots of the immunoprecipitate (IP) and supernatant (sup) fractions from DNAse I solubilized nuclei immunoprecipited with anti-pol II or anti-GFP as a negative control.

B. IGV browser screen shot of anti-pol II sense (red) and antisense (blue) tNET-seq reads at ZNF605. As expected for nascent transcripts they are enriched for intronic reads, divergent antisense reads and reads downstream of the poly(A) site.

C. IGV browser screen shot of divergent enhancer RNA (eRNA) transcription detected by anti Ser2-P tNET-seq in WT cells (top), anti-total pol II tNET-seq in WT cells (middle), anti-total pol II tNET-seq in R749H cells (lower panel). Note that these eRNA transcription units appear to be somewhat extended in the R749H mutant relative to WT similar to divergent antisense transcripts from promoters (red arrows).

D. Comparison of anti-pol II (black) and anti-Ser2P (blue) tNET-seq. IGV genome browser shots showing that anti-Ser2P tNET-seq reads are more biased toward 3′ ends (red arrows), but also have signal at 5′ ends because the entire length of the nascent RNA is sequenced.

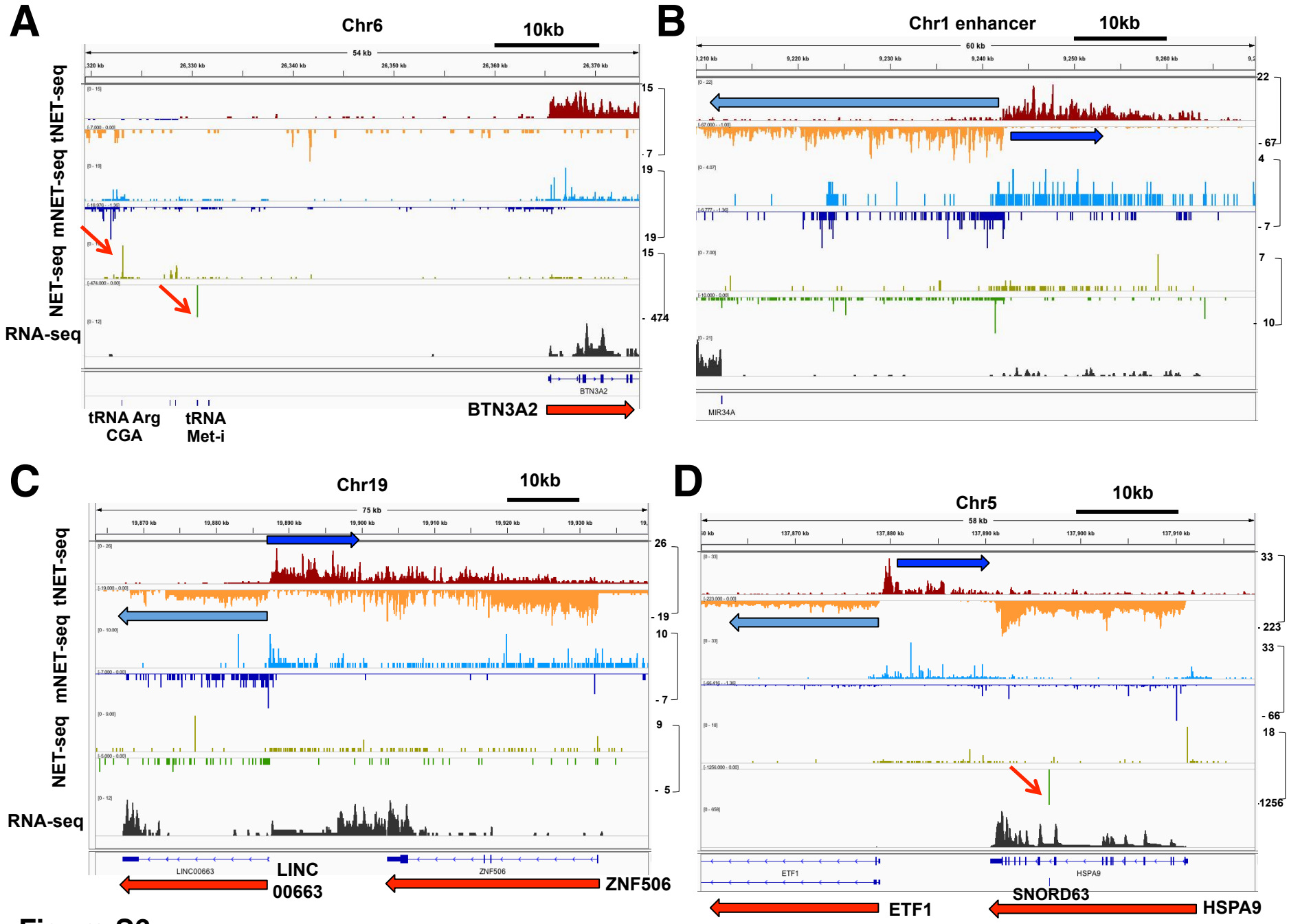
A
Chr6
10kb
NET-seq mNET-seq tNET-seq
RNA-seq
tRNA Arg CGA
tRNA Met-i
BTN3A2
B
Chr1 enhancer
10kb
MIR34A
C
Chr19
10kb
LINC00663
ZNF506
D
Chr5
10kb
ETF1
HSPA9
SNORD63

Figure S6

Figure S6. Related to Figures 5, 6.

Comparison of Nascent RNA sequencing by anti-pol II tNET-seq with 3′ end NET-seq methods.

A-D. IGV browser screen shot of strand specific NET-seq reads from anti-pol II tNET-seq in HEK293 WT Am^r cells (top panel, this study), 3′ end mNET-seq by anti- pol II 8WG16 IP in Hela cells (blue tracks, GSM1474226_ANET_8WG16_rep2) (Nojima et al., 2015) and 3′ end NET-seq of washed chromatin in HEK293 cells (green tracks, GSM1505440_HEK293T_Rep1) (Mayer et al., 2015). RNA-seq of poly A+ RNA from HEK293 WT Am^r cells (Fong et al., 2014)is shown in the bottom track. As expected nascent transcripts are enriched for intronic reads (see BTN3A2 and HSPA9 A, D), divergent antisense reads (C, D blue arrows), enhancer RNAs (B) and reads downstream of the poly(A) site (ZNF506, D) relative to RNA-seq of mature transcripts. Note that anti-pol II tNET-seq and mNET-seq samples are depleted of tRNA's (A) and mature snoRNA (D) (red arrows) relative to the chromatin NET-seq. Regions of divergent transcription are indicated with blue arrows.

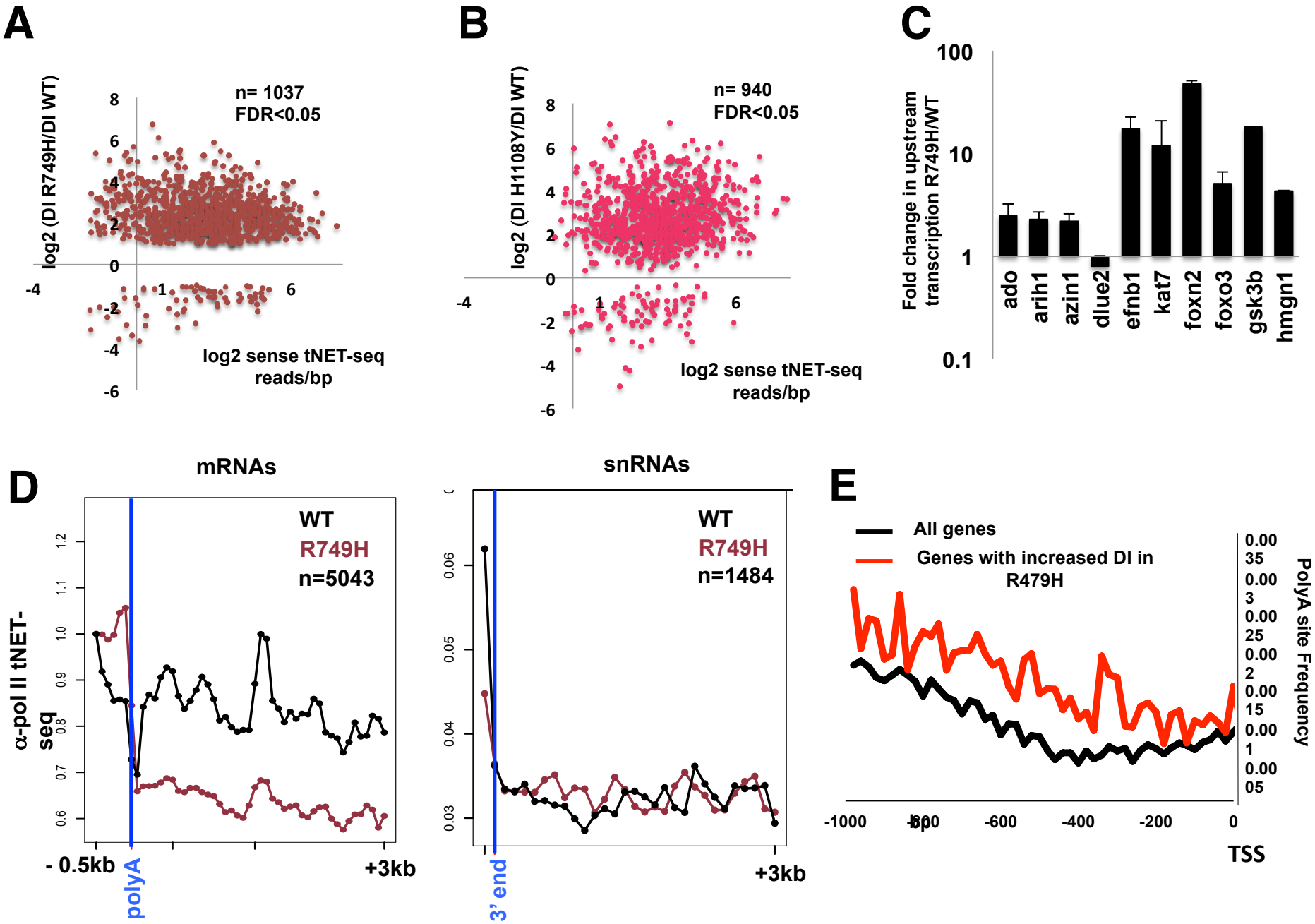
A
n= 1037
FDR<0.05
log2 (DI R749H/DI WT)
log2 sense tNET-seq reads/bp
B
n= 940
FDR<0.05
log2 (DI H1108Y/DI WT)
log2 sense tNET-seq reads/bp
C
Fold change in upstream transcription R749H/WT
ado
arih1
azin1
dlue2
efnb1
kat7
foxn2
foxo3
gsk3b
hmgn1
D
mRNAs
WT
R749H
n=5043
α-pol II tNET-seq
- 0.5kb
polyA
+3kb
snRNAs
WT
R749H
n=1484
3' end
+3kb
E
All genes
Genes with increased DI in R479H
PolyA site Frequency
TSS

Figure S7

Figure S7. Related to Figures 5, 6.

A, B. Elevated divergence index (DI) in two slow pol II mutants relative to WT. Log2 Fold change in DI for mutant/WT is plotted versus expression level measured as mean sense tNET-seq reads/bp in the region from TSS to the polyA site. DI= (divergent antisense reads (up to -5kB from TSS)/sense reads (TSS to polyA) *100). Genes analyzed are separated by >5kb upstream and those with significantly altered DI (n=3, FDR <.05, t-test) are shown.

C. Q-RT-PCR validation of increase divergent antisense transcription in R749H mutant relative to WT. Primer pairs were within 5kb upstream of the TSS normalized to divergent transcripts upstream of the MCRS1 and ACAD9 genes which were unaffected by the R749H mutant.

D. Metaplots of mean anti-pol II tNET-seq sense reads/100bp bin (n=3) at well expressed mRNA genes separated by >5kb (left panel) and snRNA genes (right panel) in WT and the R749H slow mutant. Note that unlike divergent antisense transcription from promoters, transcription by the R749H mutant does not extend further than WT at positions downstream of these genes.

E. Consensus polyA site sequences are not depleted on the antisense strand upstream of genes with elevated 5′ Ser2-P and are in fact enriched relative to all genes. The frequency of AATAAA and ATTAAA motifs was calculated using HOMER (Heinz et al., 2010)

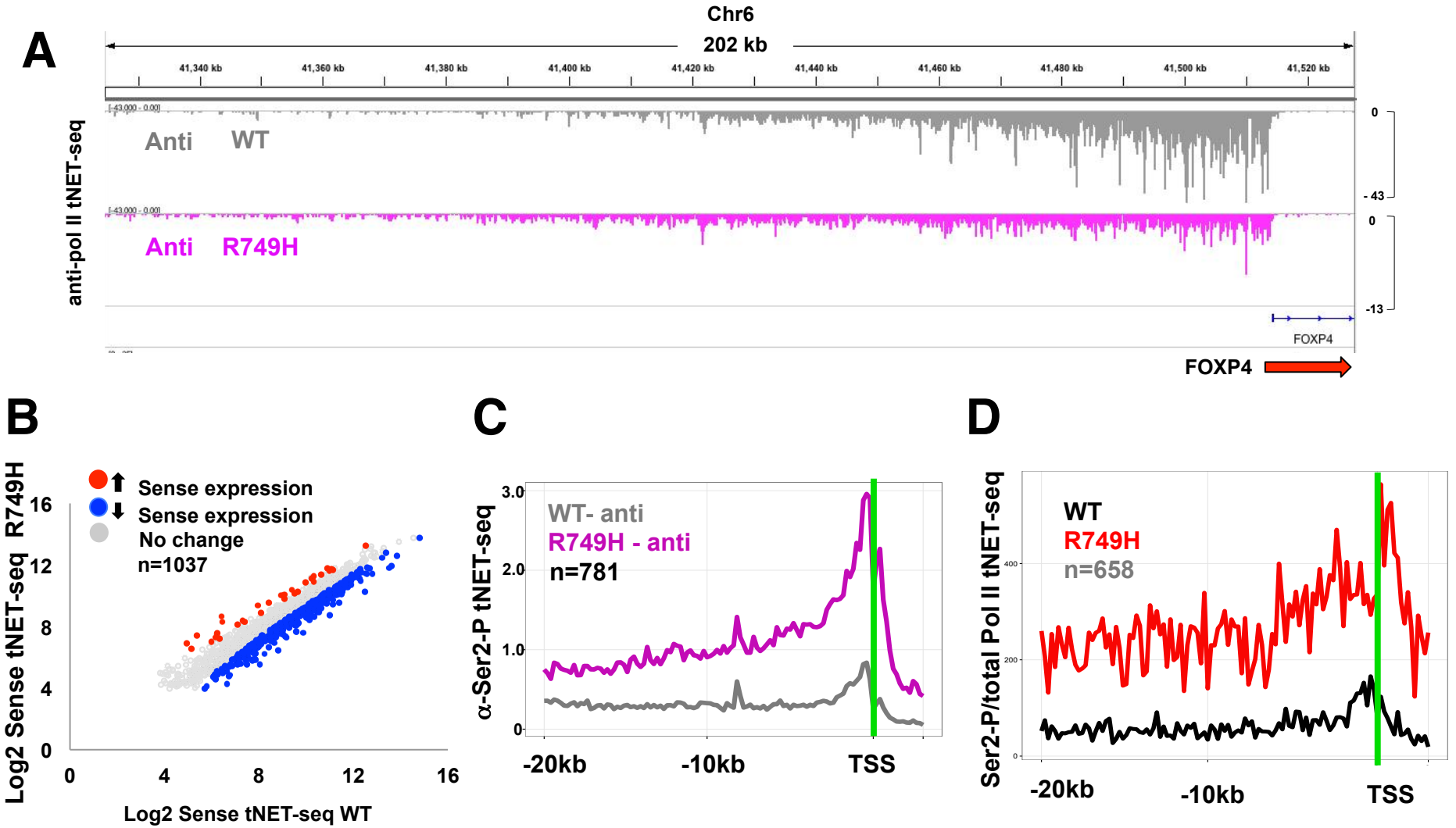
A
Chr6
202 kb
41,340 kb
41,360 kb
41,380 kb
41,400 kb
41,420 kb
41,440 kb
41,460 kb
41,480 kb
41,500 kb
41,520 kb
anti-pol II tNET-seq
Anti WT
Anti R749H
0
- 43
0
-13
FOXP4
FOXP4
B
Sense expression
Sense expression
No change
n=1037
Log2 Sense tNET-seq R749H
Log2 Sense tNET-seq WT
0
4
8
12
16
C
α-Ser2-P tNET-seq
WT- anti
R749H - anti
n=781
3.0
2.0
1.0
0
-20kb
-10kb
TSS
D
Ser2-P/total Pol II tNET-seq
WT
R749H
n=658
400
200
0
-20kb
-10kb
TSS

Figure S8

Figure S8. Related to Figure 7

A. Divergent antisense transcription of FOXP4 that produces a previously characterized PROMPT RNA (Preker et al., 2008). IGV genome browser shot of antisense anti-pol II tNET-seq reads. Note that divergent transcription by the R749H slow mutant extends further than WT.

B. Reduced sense strand nascent RNA expression on genes with significantly changed DI in R749H versus WT (see A). Genes with significantly (n=3 FDR< .05) increased and decreased sense tNET-seq signal are indicated as red and blue points. Sense strand coverage was calculated using htseq-count (Anders et al., 2015) and significant differences were calculated using DEseq2.

C. Metaplots of normalized mean anti Ser2-P tNET-seq antisense reads/200bp bin in WT and R749H slow mutant in genes with 5′ Ser2 hyperphosphorylation (Table S1). Note that the high level antisense transcription in the slow mutant extends many kilobases.

D. Elevated divergent antisense transcription by Ser2 hyperphosphorylated pol II in the slow R749H mutant. Ratios of anti Ser2-P/anti-total pol II tNET-seq signals (3 replicates) for genes with 5′ Ser2 hyperphosphorylation in the slow mutant (Table S1).

Table S1. Summary of Genes with increased 5′ Ser2-P and divergent antisense transcription in slow pol II mutants. Related to Figures 3, 5-7.

Table S2. Summary of ChIP-seq and tNET-seq seq experiments. Related to Figures 2-7

Table S3. Oligonucleotide sequences used for PCR. Related to Figure 3C.